January 2008

Shear strength model for overconsolidated clay-infilled idealised rock joints

Buddhima Indraratna
University of Wollongong, indra@uow.edu.au

M. Jayanathan
University of Wollongong

T. Brown
Golder Associates, Australia

Indraratna, B., Jayanathan, M. & Brown, E. T. (2008). *Géotechnique* **58**, No. 1, 55–65 [**doi:** 10.1680/geot.2008.58.1.55]

Shear strength model for overconsolidated clay-infilled idealised rock joints

B. INDRARATNA*, M. JAYANATHAN* and E. T. BROWN†

Saturated infilled joints can contribute to the instability of rock masses during undrained shearing. This paper reports an experimental investigation into the effect of the overconsolidation of infilled rough joints on undrained shear behaviour. A revised model is presented for predicting the shear strength of rough infilled joints on the basis of experimental tests carried out on idealised sawtoothed joints with natural silty clay as the infill material. Tests were conducted under consolidated undrained conditions in a high-pressure triaxial apparatus on joints having a dip angle of 60°. Pore pressure development in the infill materials was monitored. The results show that the effect of asperities on shear strength is significant up to a critical asperity height to infill thickness ratio (*t*/*a*), whereas the shear behaviour is controlled by the infill alone beyond this critical value. The proposed model for predicting the shear strength of rough infilled joints describes how the OCR influences the shear strength, pore water pressure development, and critical *t*/*a* ratio.

KEYWORDS: clays; consolidation; laboratory tests; pore pressures; rocks; shear strength

Des joints de remplissage saturés peuvent contribuer à l'instabilité de masses rocheuses au cours du cisaillement du sol non drainé. La présente communication rend compte des résultats d'une recherche expérimentale sur les effets de la préconsolidation de joints de remplissage grossiers sur le comportement du sol non drainé au cisaillement. On présente un modèle modifié pour la prédiction de la résistance au cisaillement de joints de remplissage grossiers, sur la base de tests expérimentaux effectués sur des joints en dents de scie idéalisés, en utilisant une argile limoneuse comme matière de remplissage. On a effectué des essais sur des sols consolidés non drainés, dans un appareil triaxial à pression élevée avec des joints présentant un angle d'inclinaison de *608*. On a contrôlé le développement de la pression interstitielle dans les matières de remplissage. Les résultats démontrent que l'effet des aspérités sur la résistance au cisaillement est significatif jusqu'à un ratio critique hauteur d'aspérité /épaisseur de remplissage (*t*/*a*), tandis que le comportement au cisaillement est contrôlé par le remplissage à lui seul, au-delà de cette valeur critique. Le modèle proposé pour la prédiction de la résistance au cisaillement de joints de remplissage grossiers décrit la façon sont l'OCR influe sur la résistance au cisaillement, le développement de la pression interstitielle de l'eau, et le rapport *t*/*a* critique.

INTRODUCTION

The presence of discontinuities in the form of joints, fractures and other planes of weakness decreases the ultimate strength and stiffness of a rock mass (e.g. Hoek, 1983; Brown, 2004). If the joints are filled with tectonically crushed rock material and/or with the products of decomposition or weathering of joints, the intact rock surfaces will not be in contact. The infill can also be transported from surface or deposition by groundwater. When the joint surfaces become weathered, the intact joint surfaces will lose contact. Therefore infilled rock joints are likely to be the weakest elements in a rock mass, and can have a dominant influence on its shear behaviour because of the low frictional properties of the infill (Jaeger, 1971; Ladanyi & Archambault, 1977; de Toledo & de Freitas, 1993; Brady & Brown, 2004). However, some infilled joints gain strength over time owing to bonding and consolidation, although these joints may be weakened again upon subsequent joint movement (Indraratna *et al*., 2005). The thicknesses of naturally occurring infills may vary from several micrometres to several metres. The wide range of parameters involved and the variety of joint and infill occurrences make it difficult to estimate the shear behaviour of infilled joints accurately.

In the past, most laboratory tests on infilled joints have been conducted under drained direct shear test conditions employing constant normal load (CNL) (e.g. Kanji, 1974; Lama, 1978; Barla *et al*., 1985; Barton, 1974; Bertacchi *et al*., 1986; Pereira, 1990; Phien-wej *et al*., 1990; de Toledo & de Freitas, 1993) or constant normal stiffness (CNS) conditions (e.g. Ohnishi & Dharmaratne, 1990; Skinas *et al*., 1990; Haberfield & Johnston, 1994; Indraratna *et al*., 1999, 2005). The infill materials used in all of these investigations may be categorised as being either cohesive (clay) or frictional (silt and sand). As reported by researchers, the shear behaviour of infilled rock joints is generally controlled by several parameters, including the parent rock and infill types, the thickness of the infill, the joint roughness, the drainage conditions, and the degree of infill overconsolidation. However, only limited studies on the effect of drainage conditions and the degree of overconsolidation have been reported in the past (e.g. Barton, 1974; de Toledo & de Freitas, 1993; Indraratna & Jayanathan, 2005).

Excess pore water pressure development, which is influenced by drainage conditions, can be expected to have a dominant influence on the shear behaviour of infilled rock joints. Several catastrophic failures of natural rock slopes in Australia have been attributed to this factor (e.g. the Kangaroo Valley rock slide, NSW, Australia; Indraratna & Ranjith, 2001). Many of the past investigations of the behaviour of infilled and unfilled rock joints in direct shear tests have been carried out under drained conditions. Limited experimental studies of the effect of pore water pressure on clean (unfilled) jointed rock specimens have been reported by Lane (1970), Goodman & Ohnishi (1973), Goodman (1976), Poirier *et al*. (1994) and Archambault *et al*. (1998, 1999), under both direct shear and triaxial undrained conditions.

Manuscript received 12 July 2006; revised manuscript accepted 16 October 2007.
Discussion on this paper closes on 1 July 2008, for further details see p. ii.
* Faculty of Engineering, University of Wollongong, Australia.
† University of Queensland, and Golder Associates Pty Ltd, Brisbane, Australia.

However, it is only recently that Indraratna & Jayanathan (2005) have reported the results of undrained triaxial tests with excess pore water pressure measurement on clay-filled model sawtoothed rock joints. They concluded that the shear strength and deformation of infilled joints are a combined effect of the joint and infill properties, the confining pressure and the drainage conditions.

It is probable that most filled or unfilled discontinuities will be in an overconsolidated or pre-loaded state when exposed at the surface. Generally, overconsolidation in fine materials occurs owing to unloading (stress relaxation), which is common in nature. For example, periodic erosion and landslides at the hilltops induce stress relief of underlying joint planes, making the infilled clayey sediments overconsolidated. A typical field situation is in Kangaroo Valley in New South Wales, Australia, where much of the groundwater-transported infill is kaolinite clayey sediments (Indraratna *et al*., 1999). Man-made excavations can also induce stress relief in rock joints. Barton (1974) reported that many hydrothermally altered infills and interbedded clay infills are mostly in an overconsolidated state. If the infilled joints remain in an undisplaced condition, the difference in shear strength between the normally and overconsolidated states may be considerable (Barton, 1974). Also, the degree of overconsolidation that many clay-infilled joints are subjected to may exceed the overconsolidation ratios (OCRs) of the natural deposits typically encountered in practice. Therefore it is expected that the stress history will have a significant influence on the peak shear strength of clay-infilled rough joints.

To investigate the overconsolidation effect and its relation to pore water pressure development, the authors have carried out a detailed laboratory testing programme on artificial overconsolidated joints with natural silty clay infill under undrained triaxial conditions. The laboratory tests were carried out on sawtoothed model rock joints with varying infill thicknesses. Although idealised triangular asperities may not resemble the undulating joint profiles encountered in the field, they nevertheless provide a simplified and reproducible basis for studying infill effects. The key objective of this study was to develop a mathematical model to predict the shear strength of clay-infilled rough joints based on effective stress test data. The proposed model captures the overconsolidation ratio (OCR) of infilled joints, in addition to the previously used measurable parameters such as the basic friction angle of the rock surfaces ϕ_b (the friction angle of a smooth planar joint), asperity angle i, the internal friction angle of the infill ϕ'_{fill}, and the infill thickness to asperity height ratio t/a.

THEORETICAL BACKGROUND

The rock joints found in nature usually have rough and undulating surfaces. Shearing of these undulating joints is resisted by their surface roughness, which may vary widely in the field. Patton (1966) described the shear strength τ of rough clean joints with regular asperities for low values of effective normal stress σ'_n as

$$\tau = \sigma'_n \times \tan(\phi_b + i) \tag{1}$$

where ϕ_b is the basic friction angle of the joint surfaces, and i is the initial asperity angle of the undulations.

Patton (1966) assumed that at low normal stress the joint was free to dilate, and that no degradation would occur during shear. With increasing normal stress, dilation is inhibited, and shearing may take place across the asperities, with degradation of the asperities occurring. In this case, the shear strength criterion must be modified to account for a new dilation angle that will be less than the initial asperity angle i. On the boundaries of underground excavations the displacement of rough discontinuities in a confined environment can be expected to cause an increase in the normal stress when dilation is prevented by the adjacent rock, promoting asperity degradation with further shearing. Under these conditions the dilation is expected to be less than that associated with the initial asperity angle. This field condition was simulated by Indraratna *et al*. (1999) using CNS test conditions. They used a Fourier function coupled with the energy consideration proposed by Seidel & Haberfield (1995) to model the shear strength of a clean joint as given by

$$(\tau_p)_{unfilled} = \left[\sigma'_{n0} + \frac{k_n}{A_j}\left(\frac{c_0}{2} + c_1 \cos\frac{2\pi h_{\tau p}}{T}\right)\right] \times \left(\frac{\tan\phi_b + \tan i}{1 - \tan\phi_b \tan i_{hp}}\right) \tag{2}$$

where σ'_{n0} is the initial effective normal stress, k_n is the normal stiffness, A_j is the joint surface area, $h_{\tau p}$ and i_{hp} are the horizontal displacement and dilation angle corresponding to the peak shear stress respectively, i is the initial asperity angle, ϕ_b is the basic friction angle, c_0 and c_1 are Fourier coefficients, and T is the period of integration of the Fourier series.

Equation (2) has to be modified if the rock joints are filled with gouge, reducing their shear strengths. Indraratna *et al*. (1999) investigated the effect of infill focusing on the shear strength of clean joints and the drop in shear strength ($\Delta\tau_p$) caused by the infill. They fitted the reduction in the normalised shear strength of infilled joints to a hyperbolic decay curve for a given t/a ratio, as shown by equation (4). The shear strength of infilled joints was estimated from equation (3) by determining the empirical hyperbolic constants δ and γ from curve-fitting of experimental data.

$$(\tau_p)_{infilled} = (\tau_p)_{unfilled} - \Delta\tau_p \tag{3}$$

where

$$\Delta\tau_p = \sigma'_{n0}\frac{t/a}{\delta \times t/a + \gamma} \tag{4}$$

It was found that the constants δ and γ were often sensitive to the infill material type, and that the hyperbolic fit was not always accurate for some types of infill, such as graphite. To predict the shear strength more accurately, Indraratna *et al*. (2005) developed a conceptual normalised shear strength model of infilled joints based on two algebraic functions, P and Q. The normalised shear strength τ_p/σ'_n was defined as the ratio between peak shear stress τ_p and the corresponding effective normal σ'_n stress on the joint surface at failure. It was assumed that the sum of P and Q gives the normalised shear strength τ_p/σ'_n for t/a ratios of less than a critical value, $(t/a)_{cr}$.

Hence for $t/a < (t/a)_{cr}$ in the region of asperity 'interference',

$$\frac{\tau_p}{\sigma'_n} = P + Q = \tan(\phi_b + i) \times (1 - k)^p + \tan\phi'_{fill} \times \left(\frac{2}{1 + 1/k}\right)^q \tag{5}$$

where $k = (t/a)/(t/a)_{cr}$, σ'_n is the effective normal stress, ϕ'_{fill} is the friction angle of the infill, and p and q are empirical constants defining the geometric loci of the functions P and Q.

In the region where $t/a > (t/a)_{cr}$ (the zone of 'non-

interference'), the shear behaviour is governed by infill alone, as the effect of the asperities is suppressed by the relatively thick infill. In this case, the normalised shear strength is estimated simply by

$$\frac{\tau_{\mathrm{p}}}{\sigma'_{\mathrm{n}}} = \tan\phi'_{\mathrm{fill}} \tag{6}$$

Although this model conveniently predicts the shear strength of infilled joints with some degree of accuracy, it requires extension to incorporate the degree of overconsolidation of the infill and so provide a more comprehensive shear strength model.

MODIFICATION OF THE SHEAR STRENGTH MODEL

The shear plane in an infilled rough joint is expected to be influenced by the t/a ratio. When the t/a ratio is less than some critical value, a part of the failure surface may propagate across the asperities, but when the t/a ratio is much greater than the critical value, the failure plane will remain within the infill itself. For smaller t/a ratios the shearing of asperities is influenced by the normal stress exerted on the joint. It is likely that for higher normal stress, when dilation will be restricted, shearing may occur through the asperities (Indraratna *et al*., 1999, 2005). In this case, some breakage of asperities will be inevitable. Different types of infill will give different critical t/a ratios, which in general exceed unity (Phien-wej *et al*., 1990; Papaliangas *et al*., 1993; Indraratna *et al*., 1999, 2005). It is also possible that the critical t/a ratio of a particular infilled joint will be influenced by its degree of overconsolidation. Fig. 1 shows the conceptual variation of the normalised shear strength ($\tau_{\mathrm{p}}/\sigma'_{\mathrm{n}}$) with t/a ratio for infilled joints having different OCR values. As shown in Fig. 1, when the OCR of the infill increases, the critical t/a ratio decreases. It is hypothesised that the critical t/a ratio of the infilled sawtoothed joints with any OCR can be expressed in terms of the OCR value n and the critical t/a ratio of the same joint with normally consolidated infill such that $(t/a)_{\mathrm{cr},n} = f[(t/a)_{\mathrm{cr},1}, \mathrm{OCR}]$, where $(t/a)_{\mathrm{cr},1}$ is the critical t/a ratio for OCR = 1, and $(t/a)_{\mathrm{cr},n}$ is the critical t/a ratio for OCR = n. To make the graphical expression of Fig. 1 convenient for modelling, a ratio $k_{\mathrm{oc},n}$ is introduced as

$$k_{\mathrm{oc},n} = \frac{(t/a)_{\mathrm{oc},n}}{(t/a)_{\mathrm{cr},n}} \tag{7}$$

where $(t/a)_{\mathrm{cr},n}$ is the critical t/a ratio of an infilled joint with an OCR of n, and $(t/a)_{\mathrm{oc},n}$ is the t/a ratio of a given infilled joint with an OCR of n.

As illustrated in Fig. 2, the shear strengths of infilled joints having varying OCRs can be classified as falling into two major zones, the *interfering* and *non-interfering* zones, on the basis of the $k_{\mathrm{oc},n}$ ratio. It is assumed that when the ratio $k_{\mathrm{oc},n}$ exceeds unity ($k_{\mathrm{oc,n}} > 1$, non-interfering), the joint behaviour becomes a function of the infill alone. Using the SHANSEP method (Ladd & Foott, 1974), an expected relation between normalised shear strength and the OCR for the infilled joints having higher infill thicknesses can be proposed, as illustrated in Fig. 3.

Hence in the region of non-interference ($k_{\mathrm{oc},n} > 1$), the normalised peak shear strength can be expressed as

$$\log\left(\tau_{\mathrm{p}}/\sigma'_{\mathrm{n}}\right)_{\mathrm{oc},n} = \log\left(\tau_{\mathrm{p}}/\sigma'_{\mathrm{n}}\right)_{\mathrm{oc},1} + \alpha\log(\mathrm{OCR}) \tag{8}$$

That is,

$$\left(\tau_{\mathrm{p}}/\sigma'_{\mathrm{n}}\right)_{\mathrm{oc},n} = \left(\tau_{\mathrm{p}}/\sigma'_{\mathrm{n}}\right)_{\mathrm{oc},1} \times \mathrm{OCR}^{\alpha} \tag{9}$$

where $(\tau_{\mathrm{p}}/\sigma'_{\mathrm{n}})_{\mathrm{oc},1}$ is the normalised shear strength of a normally consolidated infilled joint (OCR = 1), $(\tau_{\mathrm{p}}/\sigma'_{\mathrm{n}})_{\mathrm{oc},n}$ is the normalised shear strength of an infilled joint having an OCR of n, and α is an empirical constant. For normally consolidated clay the normalised shear strength can be expressed in terms of the effective shear strength parameters (Indraratna *et al*., 2005). Generally, the effective cohesion of normally consolidated clay is assumed to be zero. Therefore equation (9) can be rewritten incorporating the effective friction angle (ϕ'_{fill}) as

$$\left(\tau_{\mathrm{p}}/\sigma'_{\mathrm{n}}\right)_{\mathrm{oc},n} = \tan\phi'_{\mathrm{fill}} \times \mathrm{OCR}^{\alpha} \tag{10}$$

In the region defined by $k_{\mathrm{oc},n} < 1$, where the asperity interference is more pronounced, the previously developed shear strength model of infilled sawtoothed joints (Indraratna *et al*., 2005) is revised for the OCR value of n using the algebraic functions A_n and B_n (Fig. 2). In the case of clean

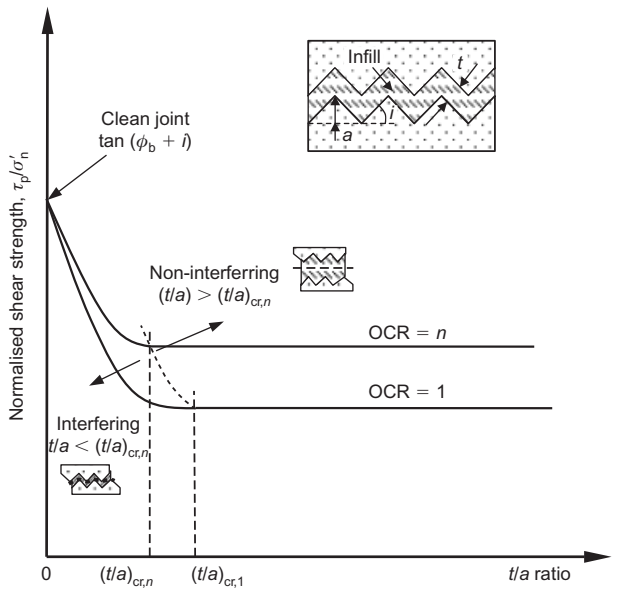

Fig. 1. Conceptual normalised shear strength variation with t/a ratio

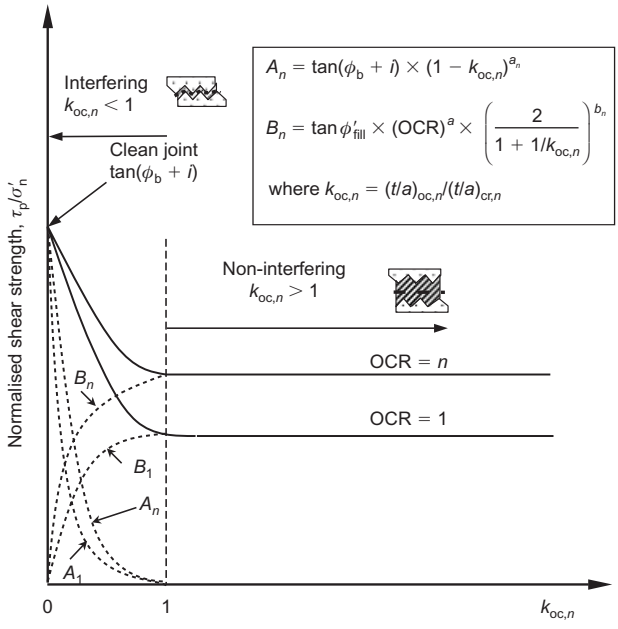

Fig. 2. Shear strength model for overconsolidated infilled idealised joints

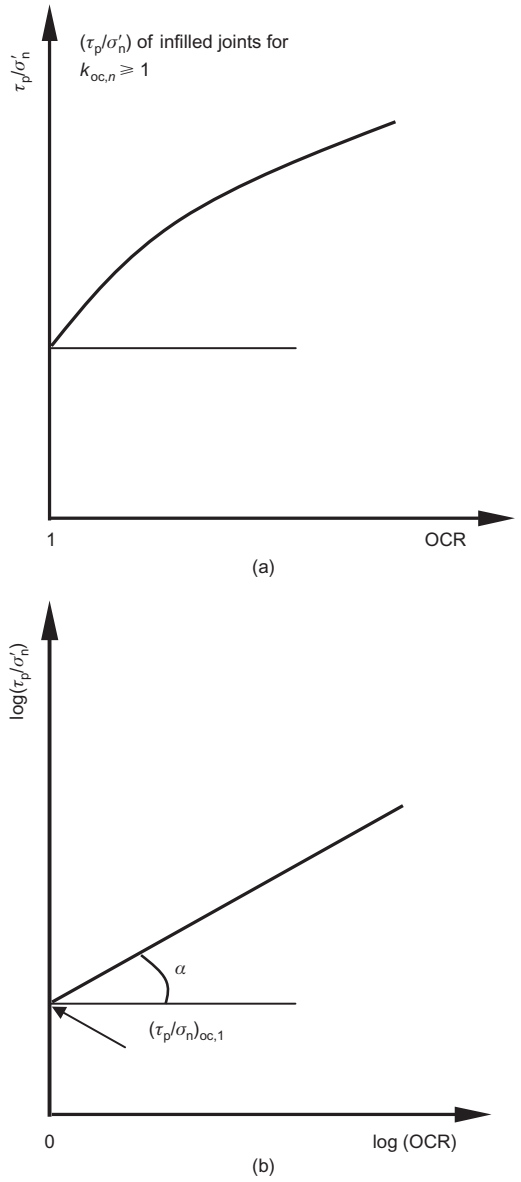

Fig. 3. Variation with OCR of normalised shear strength of infilled idealised joints for $k_{oc,n} \geqslant 1$

sawtoothed joints ($k_{oc,n} = 0$), the effect of pre-loading on (τ_p/σ'_n) is expected to be negligible. Therefore the normalised shear strength of pre-loaded or normally loaded clean joints is taken to be equal to $\tan(\phi_b + i)$, as proposed by Patton (1966). As shown in Fig. 2, the first function, A_n, is introduced to model the decrease in the influence of the $\tan(\phi_b + i)$ term with increasing $k_{oc,n}$ for an OCR of n. The second function, B_n, is used to model the gradual increase in the effect of the infill alone for the same value of OCR.

Hence for $k_{oc,n} < 1$, defining the region of asperity 'interference', the normalised peak shear strength for an OCR of n can be expressed as the sum of the two terms A_n and B_n:

$$\left(\frac{\tau_p}{\sigma'_n}\right)_{oc,n} = A_n + B_n \tag{11}$$

where

$$A_n = \tan(\phi_b + i) \times (1 - k_{oc,n})^{a_n} \tag{12}$$

and

$$B_n = \tan\phi'_{fill} \times OCR^{\alpha} \times \left(\frac{2}{1 + 1/k_{oc,n}}\right)^{b_n} \tag{13}$$

In these equations, ϕ'_{fill} is the effective friction angle of normally consolidated infill, and a_n and b_n are empirical constants defining the geometric loci of the functions A_n and B_n respectively.

As noted in this study, for infilled joints having smaller infill thicknesses ($k_{oc,n} < 1$), the overall friction angle will be influenced not only by the equivalent friction angle of an unfilled joint ($\phi_b + i$) but also by the effective friction angle of normally consolidated clay infill (ϕ'_{fill}) and the OCR. On the other hand, for the non-interfering region ($k_{oc,n} > 1$), where the effect of the basic friction angle (ϕ_b) and the roughness become negligible, the overall friction angle will be governed by the shear strength parameters of normally consolidated clay (ϕ'_{fill}) and the degree of overconsolidation. To determine the shear behaviour of a given infilled joint, the empirical constants a_n and b_n in the algebraic functions A_n and B_n, and the constant α, must be determined from the test data for a given infill, OCR and joint geometry combination. For most infilled joints, when the shear displacement increases, the shear strength may approach an ultimate or residual value, which will be considerably lower than the peak value.

LABORATORY INVESTIGATION

Preparation of model rock joints

For reasons of simplicity and reproducibility, idealised model rock joints with regular sawtoothed surfaces were cast with a mean dip angle of 60° (Indraratna & Jayanathan, 2005). Preliminary triaxial testing of unfilled joints with dip angles of 50° or less, and having 3 mm or 2 mm asperity heights, indicated that the breakage across the joints through intact material occurred owing to the high applied load needed to initiate sliding along the joint interface. It was found that the combination of a 60° dip angle and 2 mm asperity height was conducive to initiate sliding along the joint alone without any breakage across the intact material (i.e. only some breakage of asperities was observed). Therefore this combination of dip angle and asperity height was selected for all the tests in this programme. The asperity angle i of the sawtoothed joint surface was 18°. The joint profiles and the mould were machined from an acetal plastic that could be machined to any desired shape (Indraratna & Jayanathan, 2005). As shown in Fig. 4, the joint surface profile was placed in a hollow cylindrical casting mould after the application of a silicon-based lubricant to the mould and joint surfaces.

The gypsum plaster used as the casting material can be

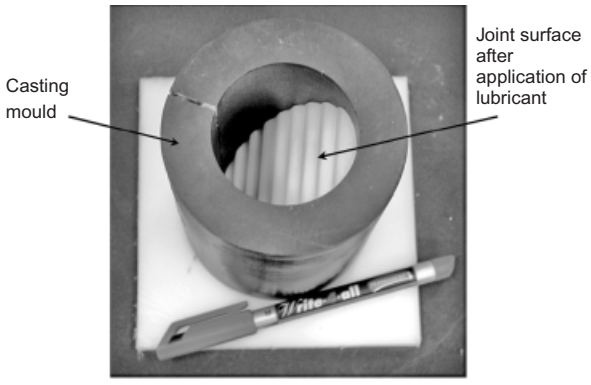

Fig. 4. Mould with joint surface profile for casting model rock joints

moulded into any shape when mixed with water, and has favourable similitude properties. This material was selected as specimens can be prepared to represent an array of sedimentary rock forms of relatively low porosity (Indraratna, 1990). Low-porosity material was preferred in this study to prevent drainage through the body of intact rock during the undrained tests (Indraratna & Jayanathan, 2005). The long-term strength of this plaster is independent of time once chemical hydration is completed. The plaster was mixed with water in a ratio of 5:3 by weight and poured into the mould with the application of a mild vibration to release any entrapped air. After being left for at least 1 h to ensure adequate hardening, the specimen was removed from the mould and cured at an oven-controlled temperature of 45°C for two weeks. Cured cylindrical specimens with a height to diameter ratio of 2 gave consistent unconfined compressive strengths σ_c of 11–13 MPa and elastic moduli E of 1·9–2·3 GPa at 50% peak strength. Shear tests on smooth planar gypsum joints gave a basic friction angle of 35°. The mechanical properties of this low-porosity model material have been reported by Indraratna (1990). A 2 mm diameter hole was drilled into the centre of the model rock joint to enable the infill material to be saturated and the pore water pressure to be measured during shear. Initial trials with two piezometer holes confirmed that the measurements from both holes were almost equal if the strain rates were low enough, justifying the use of one hole as being sufficient. Therefore testings with two holes were abandoned for the main testing programme because of concerns about the introduction of modifications to the joint geometries of the small triaxial samples.

Preparation of infilled joints

Natural gouge material collected from a rock slide site at Kangaroo Valley, NSW (170 km south of Sydney), was used as infill for the laboratory experiments. Soil tests showed that the infill could be described as a silty clay (low to moderate plasticity) with a high percentage of kaolinite. The percentages of clay and silt in this infill are approximately 24% and 42% respectively. The properties of remoulded infill measured in laboratory soil tests are listed in Table 1. As the infill recovered from the field site was clumpy, it had to be pulverised before being prepared for use as infill in the idealised laboratory joints (Indraratna & Jayanathan, 2005). The infill material was mixed with 30% water by weight using a mechanical mixer, and stored in airtight polythene bags for use during the entire experimental programme.

The jointed plaster specimens were immersed in water for at least 72 h, and subsequently an organic waterproof sealant was applied over the joint surfaces to ensure that the clay infill would be in an undrained condition during the tests. It was found that 72 h of soaking was adequate for complete saturation of the entire model joint**.** While initial soaking was to ensure saturation of the whole body of the model joint, waterproofing of joint surfaces (with a thin spray) was an added precaution to prevent any possible moisture escape during joint shearing. The basic friction angle ϕ_b of the joint surfaces was determined with a thin coating of waterproofing also: that is, all specimens have the same basic friction angle.

Table 1. Soil properties of clay infill collected from the field

Parameter	Value
Liquid limit: %	36–38
Plastic limit: %	21–22
Plasticity index: %	15–16
Coefficient of volume compressibility: m^2/MN	0·4
Compression index	0·1
Effective angle of friction: degrees	23

A 5 mm diameter porous stone tip and a filter paper were placed where the piezometer hole intercepted the joint surfaces (Indraratna & Jayanathan, 2005). The infill was then placed between the mating joint surfaces, which were assembled using a scaled 'V' block (Fig. 5). The mated joints were adjusted and trimmed to form a cylindrical test specimen containing an infilled joint having a specified infill thickness (Fig. 5). During assembly, some provision was made for the infill to accommodate the thickness reduction resulting from consolidation. Finally, the cylindrical infilled joint was wrapped in a latex membrane prior to testing. A height to diameter ratio of 2·0 and an end roughness not exceeding 0·01 mm were established according to the ISRM Suggested Method (International Society for Rock Mechanics, 1979). The detailed procedures for specimen preparation to ensure undrained conditions in the infill during shear were reported by Indraratna & Jayanathan (2005).

Testing procedure

The high-pressure two-phase triaxial apparatus at the University of Wollongong (Indraratna *et al*., 1999) was modified for use in this study. The high-strength steel triaxial cell, which can withstand internal pressures of up to 100 MPa, has an internal diameter of 100 mm and a height of 130 mm. Specimen sizes of up to 54 mm in diameter with a height to diameter ratio of 2·0 may be tested in the cell. Silicon oil was used as the confining fluid, as it prevents corrosion of the steel cell and does not react with the latex membrane. A variable constant-strain mechanical driving system was installed to apply a constant axial strain rate to the infilled joints under constant confining pressure (Indraratna & Jayanathan, 2005). The loading capacity of the driving system was 150 kN and the travel length was 120 mm. A load cell and an LVDT were used to measure the axial load and vertical displacement respectively. Pressure transducers were connected to the fluid lines to measure the confining pressure and pore pressure, and the fluid pressures were controlled by pressure controllers. All measuring devices were connected to a computer-based data-logging system for continuous data recording.

The clay-infilled jointed specimen wrapped in a latex membrane was assembled inside the modified triaxial cell. The infill was saturated by applying a back-pressure of

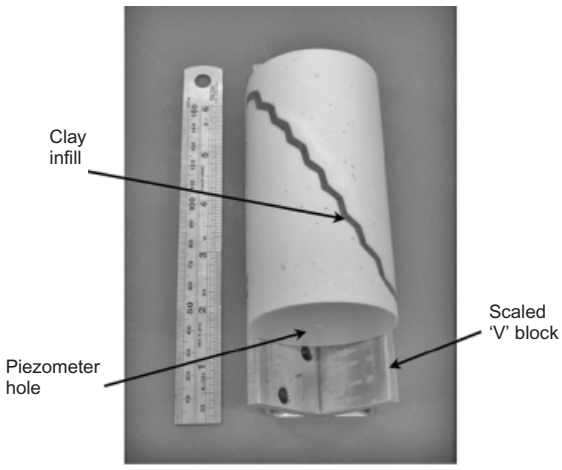

Fig. 5. Infilled idealised joint for triaxial testing

300 kPa in steps, and the degree of saturation was evaluated using Skempton's pore pressure parameter B, which was found to be in the vicinity of 0·99. The specimens were then consolidated at an elevated confining pressure. At the end of consolidation, the confining pressure was reduced to a predetermined value to achieve a specified overconsolidation ratio of the infill. Undrained tests under an effective confining pressure of 500 kPa were carried out on infilled joints having infill thickness to asperity height ratios (t/a) of between 0·5 and 5·0. Shear behaviour was investigated for infill OCRs of 1, 2, 4 and 8.

It was important to choose a shearing rate that would ensure that the pore pressures developed in the infill during shearing were equalised and measured accurately. Preliminary CNS direct shear tests carried out using two pore pressure transducers to measure pore pressures in the infill in larger specimens than those tested in the present programme showed that only at shearing speeds of less than 0·10 mm/min did the transducer measurements indicate that there was pore pressure equalisation. Accordingly, a shearing rate of 0·05 mm/min was used in the present triaxial tests on overconsolidated clay-infilled idealised joints.

EXPERIMENTAL RESULTS

In the interests of brevity, only the shear behaviour of a selected type of sawtoothed infilled joint will be presented and discussed in detail here. Plots of deviator stress and pore water pressure against axial strain for varying values of infill thickness and OCR, and the corresponding stress paths, will be elucidated.

Shear behaviour of sawtoothed joints

Figures 6(a)–6(c) show the variation of deviator stress with axial strain during shearing for normally consolidated (OCR = 1) and overconsolidated clay-filled joints with OCR = 4 and OCR = 8, for t/a ratios of 0·5, 1·0, 1·5, 2·0 and 3·5. All tests reported here were conducted at an effective confining pressure (σ'_3) of 500 kPa. The effects of increasing the confining pressure on the shear behaviour of infilled joints have been reported by Indraratna & Jayanathan (2005), and will not be discussed here. In order to establish the maximum value of the normalised shear strength shown in Fig. 2, the authors conducted a series of tests on unfilled (clean) sawtoothed joints at the same confining pressure of 500 kPa. The peak deviator stress for the clean joints of approximately 6500 kPa was several times higher than the peak values for the infilled joints shown in Figs 6(a)–6(c). However, the peak shear stress of a filled joint may be expected to approach the value for a clean joint at very low t/a and very high OCR values. Unlike the clay-filled joints, the general stress–strain responses and the peak deviator stresses of clean joints were not significantly affected by the pre-loading pressure.

For normally consolidated (OCR = 1) infilled joints, when

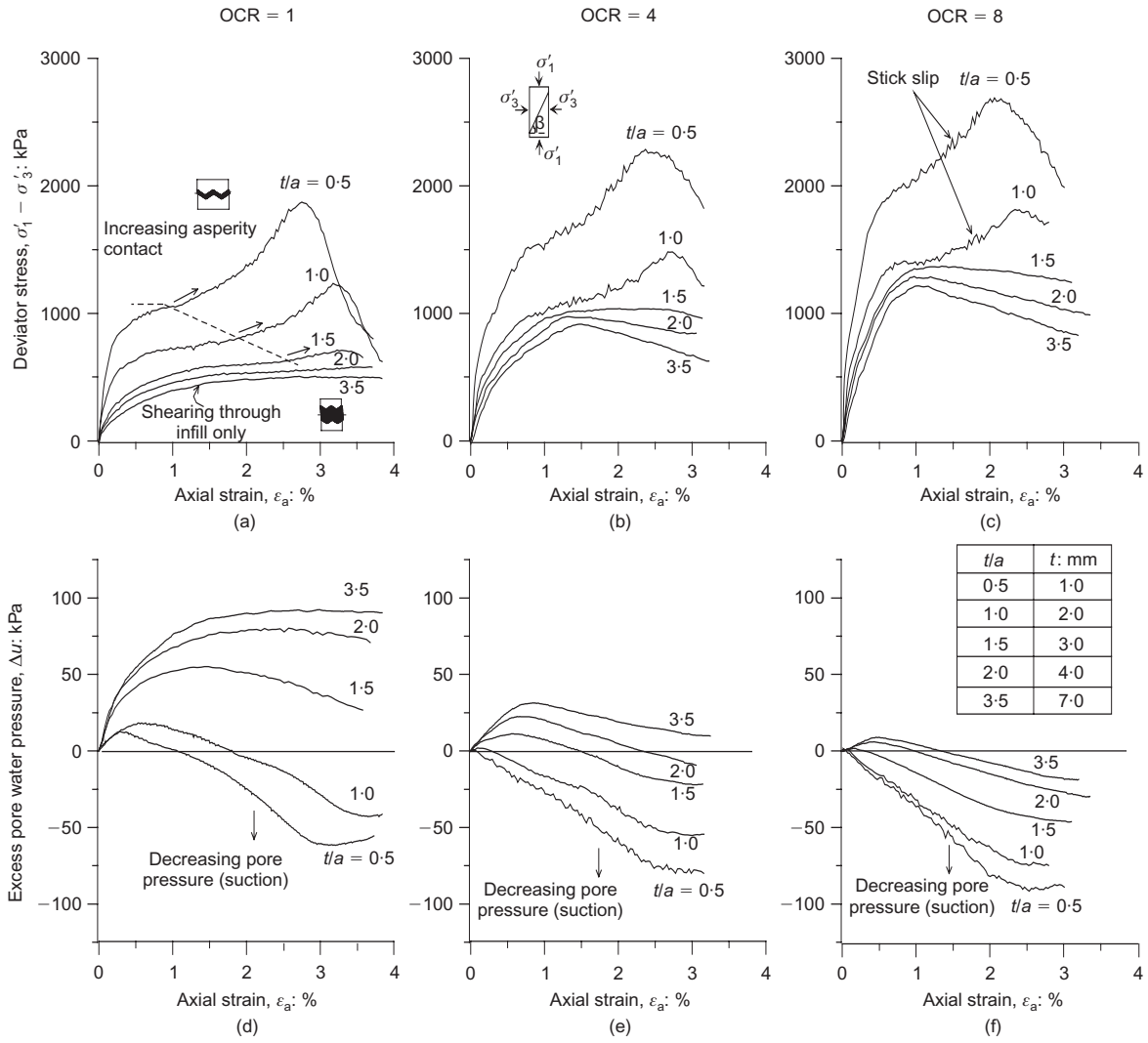

Fig. 6. Shear behaviour of infilled idealised joints with different OCR values under undrained conditions at σ'_3 = 500 kPa

$t/a \leqslant 1{\cdot}5$, the asperity interference (rock-to-rock contact) is pronounced beyond an axial strain of 1–3%, indicating a rapid rise in deviator stress (shown by the short arrows in Fig. 6(a)). The axial strain required to produce substantial asperity interference increases with increasing infill thickness. In contrast, for joints with higher infill thicknesses ($t/a > 1{\cdot}5$), the deviator stress gradually increases and attains an almost constant value, representing the typical shear behaviour of a normally consolidated clay with negligible asperity interference. When the OCR increases, for smaller infill thicknesses (e.g. $t/a = 0{\cdot}5$ and $1{\cdot}0$), the deviator stress also increases, but the axial strain required to reach the peak deviator stress decreases slightly. In the case of joints with $t/a \geqslant 1{\cdot}5$, when the OCR increases, a more distinct peak deviator stress is observed followed by a sudden stress reduction. Not surprisingly, this resembles the typical shear behaviour of an overconsolidated clay seam.

The measured changes in excess pore water pressure (Δu) are plotted against axial strain in Figs 6(d)–6(f) for t/a ratios of 0·5, 1·0, 1·5, 2·0 and 3·5. In the case of a normally consolidated (OCR = 1) clay infilled joint, for $t/a \leqslant 1{\cdot}5$ (i.e. $t \leqslant 3$ mm), the influence of joint roughness (asperities) is significant, with overriding and mating of the joint surfaces causing overall joint dilation and compression respectively. As expected, there is an increase in excess pore water pressure (Δu) of the infill upon load application, but during joint dilation Δu decreases to the negative or suction range. It is also clear that, when the infill is relatively thin ($t/a = 0{\cdot}5$), the measured suction becomes considerable for axial strains exceeding 1% (Fig. 6(d)). This is because of the relatively pronounced asperity overriding in comparison with infilled joints with $t/a \geqslant 1{\cdot}0$. For $t/a > 1{\cdot}5$ and OCR = 1, where the infill thickness is much higher (t = 4–7 mm), the pore water pressure increases to a peak and then remains relatively constant, while the deviator stress plots show ductile behaviour for strains exceeding 2%. Indraratna & Jayanathan (2005) reported that the development of pore water pressure and the associated shear behaviour are influenced by the confining pressure exerted on the joint. For overconsolidated infilled joints with smaller infill thicknesses (e.g. $t/a = 0{\cdot}5$ and $1{\cdot}0$), suction is observed even at very small strains (Figs 6(e)–6(f)). For OCR > 1 and $t/a > 1{\cdot}5$, both pore water pressure and deviator stress plots attain a peak and then fall gradually, indicating a relatively ductile response. In general, when the OCR increases, the magnitudes of the excess pore water pressures (positive) decrease (i.e. suction pressures increase). Even the joint with the thickest infill layer ($t/a = 3{\cdot}5$) sustains some suction when sheared at strains exceeding 1·5% (see the topmost curve of Fig. 6(f)).

It is of interest to note that the drop in Δu for the joints having thin infill layers (e.g. $t/a = 0{\cdot}5$ and $1{\cdot}0$) is generally associated with significant stick–slip behaviour (Figs 6(a)–6(c)). When the OCR increases, the stick–slip behaviour becomes more pronounced (e.g. Figs 6(b) and 6(c)), but this behaviour is not evident for joints having relatively higher infill thicknesses. This observed stick–slip behaviour is attributed to both asperity interference (i.e. local sliding and overriding) and some asperity degradation during shearing (Indraratna & Jayanathan, 2005). A close observation of the tested joints (joints with relatively thin infill) confirms the asperity degradation. It has been suggested that, for unfilled joints, a reduction in joint water pressure could serve to relock the joint walls and generate further stick–slip behaviour (Goodman & Ohnishi, 1973). This suggestion is supported by the observations made on clay-infilled joints in this study. Of course, the stick–slip behaviour of rock surfaces is also influenced by the relative stiffnesses of the sample and the loading system (Jaeger, 1971).

Effective stress paths

For $\sigma'_3 = 500$ kPa, effective stress paths plotted in $q = (\sigma'_1 - \sigma'_3)/2$ against $p' = (\sigma'_1 + 2\sigma'_3)/3$ space are shown in Figs 7(a)–7(c) for OCR = 1, 4 and 8 respectively. For clarity, these plots are shown only for t/a ratios of 0·5, 1·5 and 3·5. For reference, the normally consolidated (NC) and overconsolidated (OC) stress paths for the natural clay specimens (as used as infill) are also plotted as dashed lines in Fig. 7.

For $t/a = 0{\cdot}5$, the increments of p' and q are much greater owing to increased asperity contact and reduced pore water pressure. For normally consolidated infilled joints (OCR = 1), when the t/a ratio is increased from 0·5 to 1·5 or 3·5, the lengths of the pre-failure stress paths are shortened considerably, and the specimens fail at relatively small values of q. As shown in Fig. 7(a), the stress path of the specimen with $t/a = 3{\cdot}5$ is curved towards that of the normally consolidated natural clay. It is anticipated that the higher the t/a ratio, the greater will be the curvature of the corresponding stress path towards

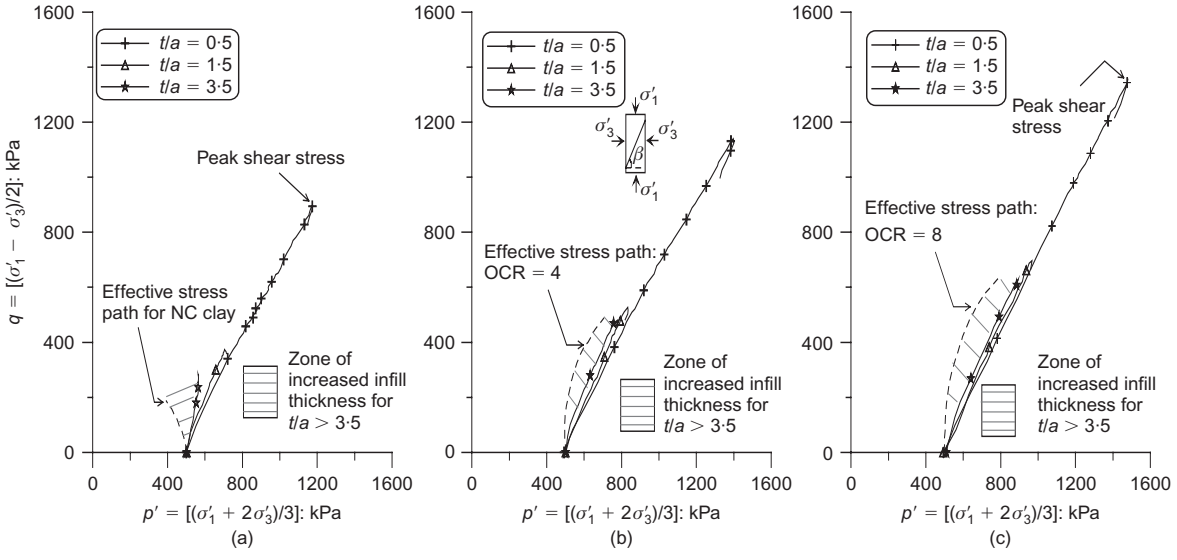

Fig. 7. Effective stress paths of infilled idealised joints: (a) OCR = 1; (b) OCR = 4; (c) OCR = 8

the normally consolidated boundary as shown by the dashed lines. As the OCR increases, the lengths of the stress paths also increase, as the specimens fail at higher values of q.

Effect of t/a ratio on τ_p/σ'_n of infilled sawtoothed joints with different OCRs

Asperity interference in infilled rough joints is usually significant at all levels of normal stress or confining pressure. However, at high infill thicknesses ($t/a > (t/a)_{cr}$) the effect of asperity interference is generally reduced. At low infill thicknesses ($t/a < (t/a)_{cr}$) the potential shear failure plane tends to intersect the rock asperities. If the applied normal stress is small, the maximum shear stress may not be large enough to shear the asperities, and the joint will then dilate and show an increase in the apparent suction (negative pore water pressure). At higher normal stresses or confining pressures, the corresponding shear stress may be large enough to break the asperities, producing a shear plane parallel to dip on which minimum dilation occurs (Indraratna & Jayanathan, 2005; Indraratna *et al*., 2005) with insignificant suction pressures developing.

Experimental verification of the normalised shear strength model

Figure 8 shows the variation of normalised peak shear strength with t/a ratio for OCR values of 1, 2, 4 and 8. The parameters used in the normalised peak shear strength (τ_p/σ'_n) calculation (the peak shear strength τ_p and the corresponding normal stress σ'_n on the joint surface) are determined by considering the point at which the maximum deviator stress is reached. For any value of OCR, when the t/a ratio is increased, τ_p/σ'_n decreases rapidly until a critical t/a ratio is reached, beyond which any further decline in τ_p/σ'_n is marginal (Fig. 8). This observation confirms the postulate that beyond this critical ratio $(t/a)_{cr}$ the shear strength is solely a function of the infill properties. For the unfilled sawtoothed joints, as the stress–strain behaviour was not governed by pre-loading, there should not be any significant change in the normalised shear strength. However, it was reported by Barton (1974) that the effect of pre-loading on unfilled tension joints may be significant owing to the interlocking of asperities. When the OCR of an infilled sawtoothed joint increases, the corresponding normalised shear strength (τ_p/σ'_n) increases and $(t/a)_{cr}$ decreases, as shown in Fig. 8.

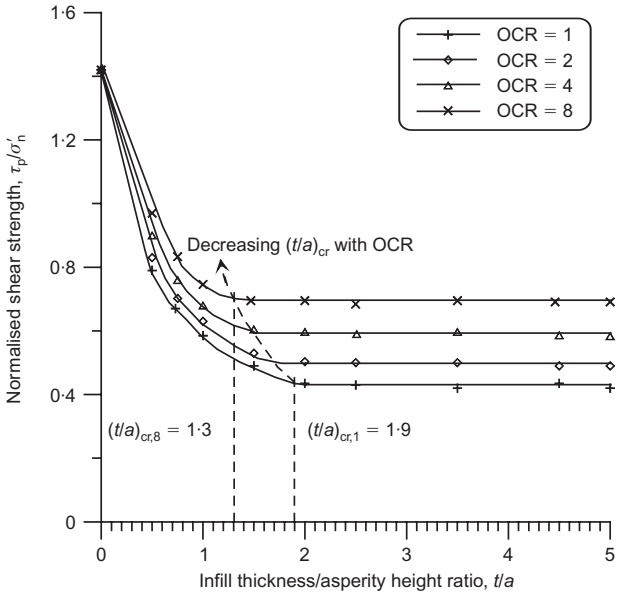

Fig. 8. Variation of normalised shear strength with *t/a* ratio for different OCRs

Based on the plot of $(t/a)_{cr}$ against OCR for infilled sawtoothed joints (Fig. 9), $(t/a)_{cr,n}$ can be related to $(t/a)_{cr,1}$ and OCR by

$$(t/a)_{cr,n} = (t/a)_{cr,1} - 0{\cdot}67 \times \log(\mathrm{OCR}) \tag{14}$$

where $(t/a)_{cr,n}$ is the critical (t/a) ratio for OCR $= n$, and $(t/a)_{cr,1}$ is the critical (t/a) ratio for normally consolidated infill (OCR $= 1$).

The results of approximately 70 undrained triaxial tests (including repeat tests) conducted on clay-infilled sawtoothed joints were used to validate the shear strength model. Test data for four different OCR values were available for joints having infill thicknesses varying from 1 mm to 10 mm, corresponding to t/a ratios of 0·5 to 5·0.

As reported by Indraratna *et al*. (2005), for normally consolidated clay-filled joints, beyond $(t/a)_{cr}$ the value of τ_p/σ'_n approaches $\tan\phi'_{fill}$. This finding is in good agreement with the undrained triaxial test data for normally consolidated joints with higher infill thicknesses ($k_{oc,1} > 1$). As illustrated earlier, the normalised shear strength (τ_p/σ'_n) of any overconsolidated joint with higher infill thickness ($k_{oc,n} > 1$) can be expressed in terms of the effective frictional angle of the infill (ϕ'_{fill}) and the OCR as

$$\left(\tau_p/\sigma'_n\right)_{oc,n} = \tan\phi'_{fill} \times \mathrm{OCR}^{0{\cdot}24} \tag{15}$$

In the case of $k_{oc,n} < 1$, the decrease in τ_p/σ'_n with increasing t/a ratio is represented well by the mathematical 'decay function' introduced in equations (11)–(13). As noted earlier, the algebraic expression A_n represents the decay of the maximum joint friction, while the term B_n models the increasing role of the infill. The normalised shear strength (τ_p/σ'_n) for $k_{oc,n} < 1$ is then given by equation (13). As shown in Fig. 10, the laboratory test data for the clay-filled sawtoothed joints with different OCRs verify the model very well. The empirical parameters a_n and b_n for different values of OCR are determined by multi-regression and are tabulated with the respective critical t/a ratios in Table 2. Indraratna *et al*. (2005) reported that the model constants a_1, b_1 and $(t/a)_{cr,1}$ depend on the roughness of the joints and the type of infill. The normalised shear strength model enables the shear strength of a given infill-joint profile combination at any t/a ratio and OCR to be determined, as long as the empirical constants a_n and b_n in equations (12) and (13) can be evaluated from the results of undrained laboratory tests. The required values of the basic friction angle of the joint

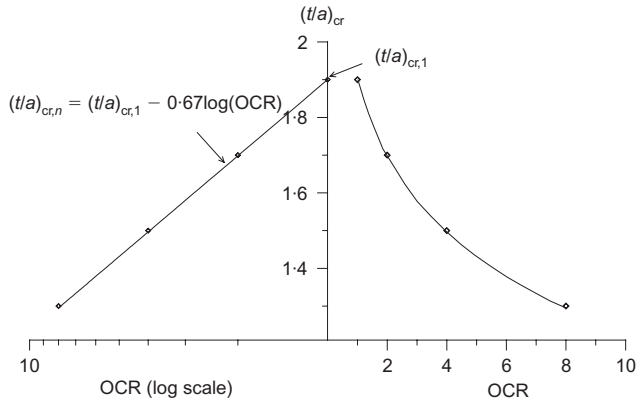

Fig. 9. Variation of critical *t/a* ratio with OCR

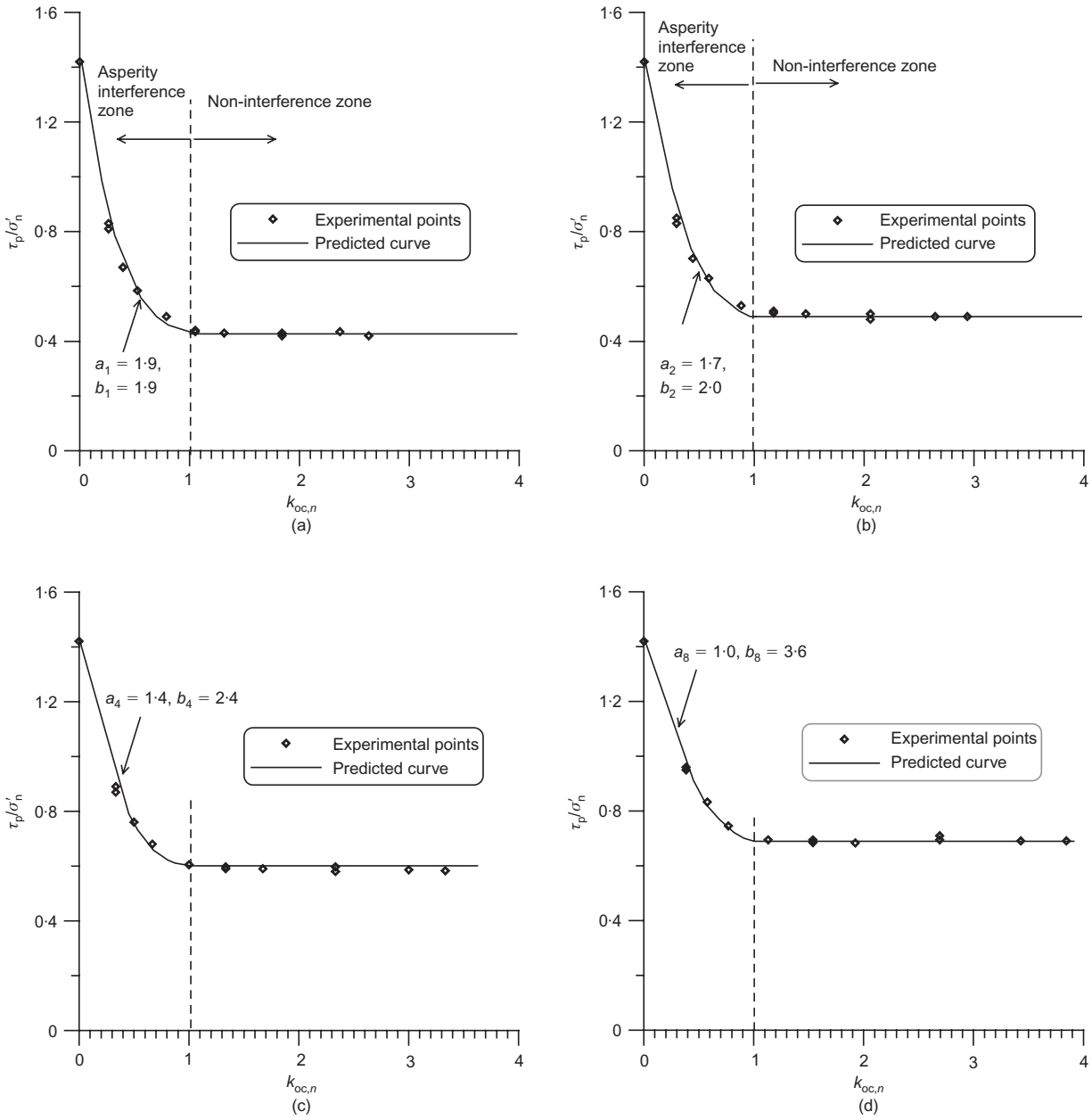

Fig. 10. Verification of shear strength model with experimental data: (a) OCR = 1; (b) OCR = 2; (c) OCR = 4; (d) OCR = 8

Table 2. Empirical constants and critical *t*/*a* ratios for different OCRs

OCR value	$(t/a)_{cr}$	a_n	b_n
1	1·9	1·9	1·9
2	1·7	1·7	2·0
4	1·5	1·4	2·4
8	1·3	1	3·6

surfaces (ϕ_b: friction angle of a smooth planar joint surface) and the angle of friction of the infill (ϕ'_{fill}) can be determined by laboratory tests, if estimates cannot be made from the available literature. The OCR can be determined from saturated consolidation tests using undisturbed infill samples collected from the field. The proposed model has been validated for sawtoothed infilled joints with OCRs of 1, 2, 4 and 8. However, further tests on different infill–joint geometry combinations with larger OCRs will further substantiate the findings of this study.

Model limitations

The proposed shear strength model incorporating OCR has a number of limitations. First, the need to carry out repetitive, reproducible tests and the requirements of simplicity justified the use of idealised sawtoothed joint profiles in the experimental programme. These profiles do not accurately represent natural joint surfaces, which are mostly irregular and wavy. Second, scale effects—that is, the effects of changes in joint surface wavelength and asperity height—were not examined. Also, coated or mineralised joints were not studied within the scope of this research programme. Finally, it is clear that the idealised sawtoothed joints with silty clay infill alone cannot represent all of the joint types and infill materials found in nature. Despite the advantages that the proposed model has over previously existing infilled joint models, its application is still constrained by the need to

perform a series of undrained triaxial tests in order to obtain the relevant empirical indices.

CONCLUSIONS

The study reported here describes the influence of infill thickness to asperity height ratio (t/a), pore pressure development, and overconsolidation ratio on the shear strength of idealised sawtoothed joints. The proposed shear strength model quantifies the reduction in the normalised shear strength observed with increasing t/a ratios at varying OCRs, and highlights the role of the critical t/a ratio, beyond which no further reduction in shear strength occurs. Despite its limitations, the model extends current understanding of the shear behaviour of infilled rock joints, with potential applications to jointed rock slope engineering and underground excavation design.

The test data demonstrate that for idealised sawtoothed joints with a thin clay infilling ($k_{\mathrm{oc},n} < 1$), the stress–strain behaviour is influenced by asperity interference, and the peak shear strength is governed by rock-to-rock contact. For increased overconsolidation, the $(t/a)_{\mathrm{cr}}$ value decreases in a predictable manner that can be quantified mathematically. For small t/a ratios ($k_{\mathrm{oc},n} < 1$), asperity overriding causes joint dilation that reduces the build-up of excess pore water pressure within the infill at any OCR value. At relatively high t/a ratios, the influence of the asperities is suppressed, in which case the responses of the infilled joints resemble those of either normally or overconsolidated clay. It is noted that the findings of the study are based on a controlled applied stress regime that only causes sliding along the joint plane with no damage to the main body of the intact rock. The proposed model has been validated only for sawtoothed joints with clay infills. Further testing of other types of infill and joint geometry at different confining pressures will be required to establish a more comprehensive database of the relevant parameters (α, a_n and b_n) to represent a wider array of joint–infill combinations.

ACKNOWLEDGEMENTS

The authors wish to acknowledge the contributions of Alan Grant (Technical Officer, University of Wollongong) during the modification of the experimental set-up and the testing programme. The second author would like to thank the Australian Government IPRS scheme and the University of Wollongong for financial support. The previous research in this area conducted by former PhD students at the University of Wollongong (Dr Asadul Haque and Dr S. Welideniya) is gratefully acknowledged.

NOTATION

A_{j}	joint surface area
A_n, B_n	components of proposed shear strength model
a	asperity height
a_n, b_n	empirical coefficients defining shape of functions A_n and B_n respectively
c_0, c_1	Fourier coefficients
h_{rp}	horizontal displacement at peak shear stress
i	initial asperity angle
i_{hp}	dilation angle at peak shear stress
k_{n}	constant normal stiffness
$k_{\mathrm{oc},n}$	ratio between $(t/a)_{\mathrm{oc},n}$ and $(t/a)_{\mathrm{cr},n}$
T	period of Fourier series
t	infill thickness
$(t/a)_{\mathrm{cr}}$	critical (t/a) ratio
$(t/a)_{\mathrm{oc},n}$	given (t/a) for OCR $= n$
$(t/a)_{\mathrm{cr,n}}$	critical t/a for OCR $= n$
Δu	excess pore water pressure
α	empirical constant
γ, δ	hyperbolic constants
σ'_{n}	effective normal stress
σ'_{n0}	initial effective normal stress
$(\tau_{\mathrm{p}}/\sigma'_{\mathrm{n}})_{\mathrm{oc},n}$	normalised peak shear strength for OCR $= n$
$(\tau_{\mathrm{p}})_{\mathrm{infilled}}$	peak shear stress of infilled joint
$(\tau_{\mathrm{p}})_{\mathrm{unfilled}}$	peak shear stress of clean joint
ϕ_{b}	basic friction angle of joint
ϕ'_{fill}	effective friction angle of normally consolidated infill

REFERENCES

Archambault, G., Poirier, S., Rouleau, A., Gentier, S. & Riss, J. (1998). The behaviour of induced pore fluid pressure in undrained triaxial shear test on fracture porous analog rock material specimens. In *Mechanics of jointed and faulted rock* (ed. H. R. Rossmanith), pp. 583–589. Rotterdam: Balkema.

Archambault, G., Poirier, S., Rouleau, A., Gentier, S. & Riss, J. (1999). Pore pressure behaviour in undrained triaxial shear tests on joints. *Proc. 9th Congr. Int. Soc. Rock Mech., Paris* **1**, 741–746.

Barla, G., Forlati, F. & Zaninetti, A. (1985). Shear behaviour of filled discontinuities. *Proceedings of the international symposium on fundamentals of rock joints*, Bjorkliden, pp. 163–172.

Barton, N. (1974). *Review of shear strength of filled discontinuities in rock*. Publication No. 105. Oslo: Norwegian Geotechnical Institute.

Bertacchi, P., Zaninetti, A., Barla, G. & Forlati, F. (1986). Laboratory tests on the shear behaviour of filled discontinuities. *Proceedings of the international symposium on* Engineering in Complex Rock Formations, Beijing, pp. 262–270.

Brady, B. H. G. & Brown, E. T. (2004). *Rock mechanics for underground mining*, 3rd edn. Dordrecht: Kluwer Academic Publishers.

Brown, E. T. (2004). The mechanics of discontinua: engineering in discontinuous rock masses. John Jaeger Memorial Lecture. *Proc. 9th Australia New Zealand Conf. on Geomech., Auckland* **1**, 51–72.

de Toledo, P. E. C. & de Freitas, M. H. (1993). Laboratory testing and parameters controlling the shear strength of filled rock joints. *Géotechnique* **43**, No. 1, 1–19.

Goodman, R. E. (1976). *Methods of geological engineering.* St Paul: West Publishing Co.

Goodman, R. E. & Ohnishi, Y. (1973). Undrained shear testing of jointed rock. *Rock Mech.* **5**, No. 3, 129–149.

Haberfield, C. M. & Johnston, I. W. (1994). A mechanistically based model for rough rock joints. *Int. J. Rock. Mech. Min. Sci. Geomech. Abstr.* **31**, No. 4, 279–292.

Hoek, E. (1983). Twenty-third Rankine Lecture: Strength of jointed rock masses. *Géotechnique* **33**, No. 3, 187–223.

Indraratna, B. (1990). Development and applications of a synthetic material to simulate soft sedimentary rocks. *Géotechnique* **40**, No. 2, 189–200.

Indraratna, B. & Jayanathan, M. (2005). Measurement of pore water pressure of clay-filled rock joints during triaxial shearing. *Géotechnique* **55**, No. 10, 759–764.

Indraratna, B. & Ranjith, P. (2001). Laboratory measurement of two-phase flow parameters in rock joints based on high pressure triaxial testing. *J. Geotech. Geoenviron. Engng ASCE* **127**, No. 6, 530–542.

Indraratna, B., Haque, A. & Aziz, N. (1999). Shear behaviour of idealized infilled joints under constant normal stiffness. *Géotechnique* **49**, No. 3, 331–355.

Indraratna, B., Welideniya, H. S. & Brown, E. T. (2005). A shear strength model for idealised infilled joints under constant normal stiffness (CNS). *Géotechnique* **55**, No. 3, 215–226.

International Society for Rock Mechanics (1979). Suggested methods for determining the uniaxial compressive strength and deformability of rock materials. *Int. J. Rock Mech. Min. Sci*. **16**, No. 2, 135–140.

Jaeger, J. C. (1971). Eleventh Rankine Lecture: Friction of rocks and stability of rock slopes. *Géotechnique* **21**, No. 2, 97–134.

Kanji, M. A. (1974). Unconventional laboratory tests for the determination of the shear strength of soil-rock contacts. *Proc. 3rd Congr. Int. Soc. Rock Mech*., *Denver* **2**, 241–247.

Ladanyi, B. & Archambault, G. (1977). Shear strength and deformability of filled indented joints. *Proc. 1st Int. Symp. on Geotechnics of Structurally Complex Formations, Capri*, 317–326.

Ladd, C. C. & Foott, R. (1974). New design procedure for stability of soft clays. *J. Geotech. Engng ASCE* **100**, No. GT7, 763–786.

Lama, R. D. (1978). Influence of clay fillings on shear behaviour of joints. *Proc. 3rd Congr. Int. Assoc. Engng Geol., Madrid* **2**, 27–34.

Lane, K. S. (1970). Engineering problem due to fluid pressure. *Rock Mechanics: Theory and Practice*, *Proc. 10th US Symp. Rock Mech., Berkeley*, 501–540.

Ohnishi, Y. & Dharmaratne, P. G. R. (1990). Shear behaviour of physical models of rock joints under constant normal stiffness conditions. *Proceedings of the international conference on rock joints, Loen* (ed. N. R. Barton, & O. Stephansson), pp. 267–273. Rotterdam: Balkema.

Papaliangas, T., Hencher, S. R., Lumsden, A. C. & Manolopoulou, S. (1993). The effect of frictional fill thickness on the shear strength of rock discontinuities. *Int. J. Rock Mech. Min. Sci. Geomech. Abstr.* **30**, No. 2, 81–91.

Patton, F. D. (1966). Multiple modes of shear failure in rocks. *Proc. 1st Congr. Int. Soc. Rock Mech., Lisbon* **1**, 509–513.

Pereira, J. P. (1990). Mechanics of filled discontinuities. In *Mechanics of jointed and faulted rock* (ed. H. P. Rossmanith), pp. 375–380. Rotterdam: Balkema.

Phien-wej, N., Shrestha, U. B. & Rantucci, G. (1990). Effect of infill thickness on shear behaviour of rock joints. *Proceedings of the international conference on rock joints, Loen* (eds N. R. Barton & O. Stephansson), pp. 289–294. Rotterdam: Balkema.

Poirier, S., Archambault, G. & Rouleau, A. (1994). Experimental testing of pore water influences on physico-mechanical properties of a porous rock analog material. *Proc. 47th Can. Geotech. Conf., Halifax*, 418–427.

Seidel, J. P. & Haberfield, C. M. (1995). The application of energy principles to the determination of the sliding resistance of rock joints. *Rock Mech. Rock Engng* **28**, No. 4, 211–226.

Skinas, C. A., Bandis, S. C. & Demiris, C. A. (1990). Experimental investigations and modelling of rock joint behaviour under constant stiffness. *Proceedings of the international conference on rock joints, Loen* (eds N. R. Barton & O. Stephansson), pp. 301–307. Rotterdam: Balkema.